

## Reconstruction Effects on Surface Properties of Co/Mg/Al Layered Double Hydroxide

Denis SOKOL<sup>1</sup>, Kristina KLEMKAITE-RAMANAUSKE<sup>2</sup>, Alexander KHINSKY<sup>2</sup>, Kestutis BALTAKYS<sup>3</sup>, Aldona BEGANSKIENE<sup>1</sup>, Arunas BALTUSNIKAS<sup>4</sup>, Jiri PINKAS<sup>5,6</sup>, Aivaras KAREIVA<sup>1\*</sup>

<sup>1</sup> Department of Inorganic Chemistry, Vilnius University, Naugarduko 24, LT-03225 Vilnius, Lithuania

<sup>2</sup> Amiagus, A. Mackeviciaus 50, LT-44258, Kaunas, Lithuania

<sup>3</sup> Department of Silicate Technology, Kaunas University of Technology, Radvilėnų 19, LT-50254 Kaunas, Lithuania

<sup>4</sup> Materials Research and Testing Laboratory, Lithuanian Energy Institute, Breslaujos 3, LT-44403 Kaunas, Lithuania

<sup>5</sup> Department of Chemistry, Masaryk University, Kotlarska 267/2, CZ-61137 Brno, Czech Republic

<sup>6</sup> CEITEC MU, Masaryk University, Kamenice 753/5, CZ-62500 Brno, Czech Republic

crossref <http://dx.doi.org/10.5755/j01.ms.23.2.15184>

Received 06 June 2016; accepted 19 November 2016

Layered double hydroxides having different cationic ( $\text{Mg}^{2+}$ ,  $\text{Co}^{2+}$ ,  $\text{Al}^{3+}$ ) composition were successfully synthesized by the low supersaturation method. The samples were thermally decomposed and reconstructed using water and nitrate media at different temperatures. X-ray powder diffraction analysis, X-ray fluorescence analysis, thermogravimetry and BET/BJH methods were used to investigate the differences between the directly obtained layered materials and those after the reconstruction process.

**Keywords:** layered double hydroxide, Mg/Co/Al, reconstruction effect, mixed-metal oxide, BET, BJH.

### 1. INTRODUCTION

Layered double hydroxides (LDHs) are the commonly used names to describe a class of layered materials based on the brucite  $\text{Mg}(\text{OH})_2$  crystal structure and having a general chemical formula of  $[\text{M}^{\text{II}}_{1-x}\text{M}^{\text{III}}_x(\text{OH})_2]^{x+}(\text{A}^{\text{m}})_{x/m}\cdot n\text{H}_2\text{O}$  [1, 2]. LDHs can be prepared with different divalent and trivalent cations in the structure and serve as precursors for the preparation of mixed metal oxides used as catalysts. The exact features, such as the nature of the cations in the brucite-like layers and the specific surface area have a significant effect on their final catalytic properties. In the past decades, a number of cobalt containing LDHs, where  $\text{Mg}^{2+}$  is replaced by  $\text{Co}^{2+}$ , have been prepared [3–9]. The obtained Co/Mg/Al LDHs showed a unique layered structure. The evolution of the lattice parameter  $a$  with the cations  $\text{Co}^{2+}$ ,  $\text{Mg}^{2+}$ , and  $\text{Al}^{3+}$  composition provided evidence that they are combined in the same layer. The crystallinity of LDHs showed dependents on the amount of  $\text{Co}^{2+}$  and/or  $\text{Mg}^{2+}$ , probably due to their respective ion radii. The isomorphous replacement of  $\text{Co}^{2+}$  by  $\text{Mg}^{2+}$  showed effect on the amount of water in the interlayer due to the well-known ability of these cations to be hydrated. A higher thermal stability of samples containing a low amount of cobalt were explained by the higher local charge density of the layers or by the higher affinity of  $\text{Mg}^{2+}$  towards  $\text{CO}_3^{2-}$ .

Calcined Co/Mg/Al LDHs form  $\text{Co}_x\text{Mg}_{1-x}\text{Al}_2\text{O}_4$  solid solutions having the spinel structure and various cations distributions. Depending on the nature of cations and the

temperature of activation, the formation of monophasic solid solutions with rock salt or spinel-like structures or segregation of several phases was also observed [10–12]. The Co/Mg/Al LDHs showed different decomposition profiles compared to the binary compositions. Thermogravimetric analysis showed two mass losses corresponding to the dehydration and dehydroxylation/deanionation. The decomposition temperature of Co/Mg/Al system was reported to be higher than that of Co/Al LDHs but lower than Mg/Al LDHs [9].

Detailed reconstruction studies, however, are practically limited to the Mg/Al systems. It has just been shown that Co/Al LDHs do not easily recover the original structure [9, 13–15]. It has been shown that the Co/Mg/Al system with lower loadings of cobalt forms only Mg(Al)O mixed oxide phase after calcination at 1023 K, avoiding the spinel formation which could influence the reformation of LDHs with cobalt in the structure. Cobalt mixed oxide Co/Mg/Al supported on calcined hydrotalcite was obtained by dipping calcined Mg–Al hydrotalcite in a cobalt nitrate aqueous solution [16–18]. This compound was used as catalysts for the total oxidation of toluene.

The LDHs are widely used in commercial products as adsorbents, catalyst support precursors, anion exchangers, acid residue scavengers, flame retardants, polymer stabilizers, osmosis membranes, sensors and so on [19–22].

Investigation of mixed oxides derived from calcined LDHs prepared by direct and indirect methods is an interesting topic, since the reformation media could have an effect not only on the composition of a solid but also on the morphology of oxides. In this study, the synthesis by co-precipitation method at low supersaturation was chosen

\* Corresponding author: Tel +370 5 2193110.

E-mail address: [aivaras.kareiva@chf.vu.lt](mailto:aivaras.kareiva@chf.vu.lt) (A. Kareiva)

as a direct route to prepare Co/Mg/Al LDH materials. The synthesized LDHs were thermally decomposed and following the indirect method, they were reconstructed. The surface area and porosity as important characteristics of these materials were investigated in this study in detail.

## 2. EXPERIMENTAL

For the synthesis of LDHs  $\text{Al}(\text{NO}_3)_3 \cdot 9\text{H}_2\text{O}$ ,  $\text{Mg}(\text{NO}_3)_2 \cdot 6\text{H}_2\text{O}$ ,  $\text{Co}(\text{NO}_3)_2 \cdot 6\text{H}_2\text{O}$ , NaOH,  $\text{NaHCO}_3$  from Lach-Ner, s.r.o. (Neratovice, Czech Republic) were used. Deionised water was used for all syntheses, solution preparations and washing of synthesis products. LDHs were prepared by the coprecipitation under low supersaturation from a solution of the appropriate metal nitrates with a molar ratio of  $(\text{Co} + \text{Mg}):\text{Al} = 3:1$  and a solution of  $\text{NaHCO}_3:\text{NaOH}$  with a molar ratio of 1:2. During the preparation, 15 % of the  $1 \text{ mol L}^{-1} \text{Mg}(\text{NO}_3)_2$  solution was replaced by a  $1 \text{ mol L}^{-1} \text{Co}(\text{NO}_3)_2$  solution. The solution of metal nitrates was added very slowly to the solution of  $\text{NaHCO}_3 + \text{NaOH}$  ( $\text{pH} \approx 12$ ) under vigorous stirring. After mixing the obtained gel was aged at 353 K for 6 h. The slurry was filtered and washed with distilled water and dried in open air. The resulting powder was marked as Co/Mg/Al. The mixed-metal oxide obtained by subsequent heating at 923 K for 3 h was labelled as Co/Mg/Al<sub>cal</sub>. The reconstruction of LDHs from Co/Mg/Al<sub>cal</sub> was performed in water at  $\text{pH} \approx 6$  (2 g of mixed oxide in 40 mL of water) and in magnesium nitrate solution at  $\text{pH} \approx 3.7$  (2 g of mixed oxide in 40 mL of  $1 \text{ mol L}^{-1} \text{Mg}(\text{NO}_3)_2$ ) at 293 K and 353 K for 6 h. The samples reconstructed in water were labelled as Co/Mg/Al<sub>W293</sub>, Co/Mg/Al<sub>W353</sub> and the specimens reconstructed in nitrate media were named as Co/Mg/Al<sub>N293</sub>, Co/Mg/Al<sub>N353</sub>. After the reconstructed processes, the samples were washed with water and dried in air. Schematic presentation of synthesis and post-synthesis modifications of LDH samples is shown in Fig. 1.

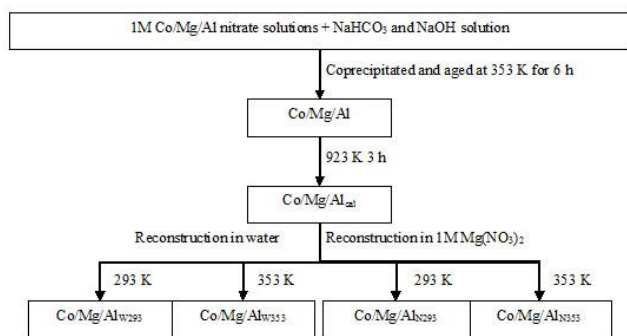


**Fig. 1.** Flow-chart of synthesis and post-synthesis modifications of LDH samples

The influence of the reconstruction conditions on the specific surface area, pore volume and pore size distribution were investigated after thermal treatment in air at 923 K for 3 h using nitrogen adsorption/desorption isotherms. The specific surface area was evaluated by the Brunauer-Emmet-Teller method (BET) [23] and the pore-size distribution by the Barret-Joyner-Halenda (BJH) procedure [24]. Prior to analysis, the calcined cobalt containing LDHs were outgassed at 523 K for 5 h. The

measurements were carried out on a Quantachrome Autosorb-1MP instrument using the program Autosorb. The specific surface area was also calculated using two models (cylinder pores and pores between parallel plates) and compared to experimentally obtained specific surface area. The calculation was made according to [25]. The X-ray powder diffraction (XRD) patterns of the synthesized, calcined and reconstructed LDH samples were recorded with a conventional Bragg-Brentano geometry ( $\theta - 2\theta$  scans) on a DRON-6 automated diffractometer, equipped with a secondary graphite monochromator. Cu  $K_\alpha$  radiation ( $\lambda = 1.541838 \text{ \AA}$ ) was used as a primary beam. The patterns were recorded from  $5$  to  $70^\circ 2\theta$  in steps of  $0.02^\circ 2\theta$ , with the measuring time of  $0.5 \text{ s}$  per step. Silicon was used as a reference sample. The cell parameters  $a$  and  $c$  of the rhombohedral structure were determined from the positions of the (110) and (003), (006) diffraction lines, respectively. The lattice parameter  $a = 2d(110)$  corresponds to an average cation-cation distance calculated from the 110 reflection, while the  $c$  parameter corresponds to three times the thickness of  $d(003)$  parameter. In this case  $c$  was calculated from two diffraction lines using equation  $c = 3/2 [d(003) + 2d(006)]$ . Thermogravimetric (TG) analysis of Co/Mg/Al samples was carried out with a Netzsch STA 409 PC Luxx instrument using a heating rate of  $10 \text{ K/min}$  in air atmosphere. Metal loadings of the LDHs were analyzed by X-ray fluorescence technique (XRF) on a Spectro Analytical Instrument GmbH&Co.KG spectrometer with a Pd window X-ray tube. Mean values of relative standard deviation for analysed elements were 1.54 % for Mg, 1.42 % for Al and 3.7 % for Co.

## 3. RESULTS AND DISCUSSION

The XRD patterns of synthesized, decomposed and reconstituted LDHs are shown in Fig. 2.

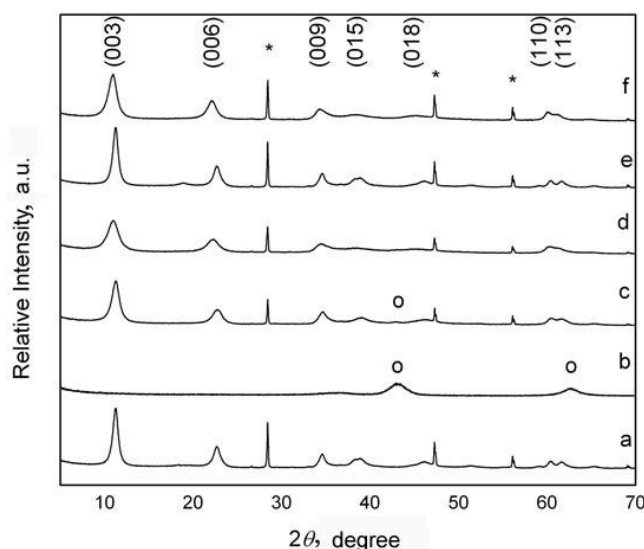


**Fig. 2.** XRD patterns of synthesized, decomposed and reconstructed LDHs: a – Co/Mg/Al; b – Co/Mg/Al<sub>cal</sub>; c – Co/Mg/Al<sub>W293</sub>; d – Co/Mg/Al<sub>N293</sub>; e – Co/Mg/Al<sub>W353</sub>; f – Co/Mg/Al<sub>N353</sub>. Additional phases are marked: o – MgO and \* – Si used as a reference

The characteristic hydroxalite type structure of as-synthesized sample Co/Mg/Al was confirmed by the XRD analysis data (Fig. 2 a) [7, 10]. Intensive and sharp reflections of the (003) and (006) planes at low  $2\theta$  values ( $11-23^\circ$ ), and broad asymmetric reflections at higher  $2\theta$  values ( $34-66^\circ$ ) can be observed. The calculated cell parameter  $c = 23.6 \text{ \AA}$  (Table 1) for the synthesized LDH sample is slightly higher compared to the published value of  $23.4 \text{ \AA}$  for carbonate-containing Mg/Al LDHs [26]. After thermal decomposition only two broad reflections located at around  $2\theta = 43-44^\circ$  and  $62-63^\circ$  are seen in the XRD pattern (Fig. 2 b). The XRD analysis of heat-treated sample revealed the formation of poorly crystalline magnesium oxide (PDF # 75-1525). No reflections of cobalt or aluminium oxides were observed. Moreover, the XRD patterns of calcined samples do not show the formation of spinel-type crystalline phases.

To reconstruct the LDHs, the mixed metal oxides were immersed in water or magnesium nitrate solutions to restore the layered structure. An influence of media temperature on the reconstruction effect was also investigated. The XRD patterns of LDH samples obtained after the hydration process at 293 and 353 K are given in Fig. 2 c and Fig. 2 e, respectively. At room temperature, an incomplete regeneration was observed in water since a weak MgO reflections were present in the XRD pattern. Interestingly, this oxide phase disappeared when the reconstruction process was carried out at higher temperature (353 K), suggesting the significance of the medium temperature on the reformation of LDHs. The XRD patterns of mixed oxides after treatment in a  $\text{Mg}(\text{NO}_3)_2$  solution at 293 and 353 K are given in Fig. 2 d and Fig. 2 f, respectively. The XRD patterns of LDH reconstructed in magnesium nitrate solution are slightly different in comparison with those of as-synthesized (Fig. 2 a) and reformed in water (Fig. 2 c and e). The 003 reflection is shifted to a lower  $2\theta$  angle for both samples, indicating that the interlayer region is expanded by the intercalation of a larger anion, which is most likely nitrate. Obvious decrease of intensity and broadening of reflections can be also observed. The reformation in the magnesium nitrate solution has the strongest effect on the  $c$  parameter of LDHs (Table 1).

**Table 1.** Crystallographic data and crystallite size of synthesized and reconstructed LDHs

Sample	$d_{003}$	$d_{006}$	$d_{110}$	Cell parameters, $\text{\AA}$		Crystallite size, $\text{\AA}$
				$c$	$a$	
Co/Mg/Al	7.93	3.92	1.53	23.60	3.07	61
Co/Mg/Al <sub>w293</sub>	7.88	3.90	1.53	23.52	3.06	91
Co/Mg/Al <sub>N293</sub>	8.08	3.99	1.53	24.10	3.07	61
Co/Mg/Al <sub>w353</sub>	7.89	3.91	1.53	23.57	3.06	131
Co/Mg/Al <sub>N353</sub>	8.12	4.01	1.54	24.22	3.08	80

The basal spacing represents the thickness of a single layer and is normally related to the size of charge balancing interlayer anions. For the samples reconstructed in the magnesium nitrate solution, the  $d_{003}$  values are higher than  $8 \text{ \AA}$ .

Thermogravimetric analysis was performed on as-synthesized Co/Mg/Al LDH (Fig. 3). Evidently, three

typical mass loss steps can be observed in the TG curve associated with the removal of interlayer and adsorbed water, the elimination of the interlayer structural water and finally the dehydroxylation and decarbonation [26]. As seen in Fig. 3, the endothermic processes of water removal continue until 523 K and two DTG minima at 360 K and 493 K could be determined. The coupling of dehydroxylation and decarbonation processes can be observed because of the single mass loss in the temperature range of 523–773 K. The presence of cobalt in the synthesized LDH sample showed a very minor effect on the thermal behaviour of LDH comparable to previous results reported on Ni/Mg/Al LDHs [27]. According to the TG results, the temperature of 923 K was chosen for full decomposition of LDH. The annealing temperature is very important because it is crucial for a successful reconstruction of the layered structure. During the calcination of LDHs, the temperature should be higher than the layer collapse point but lower than the formation temperature of the spinel phase. This solid phase is stable and cannot be converted back to LDHs in water. Thus, for LDHs the calcinations temperature is usually set between 673 and 973 K.

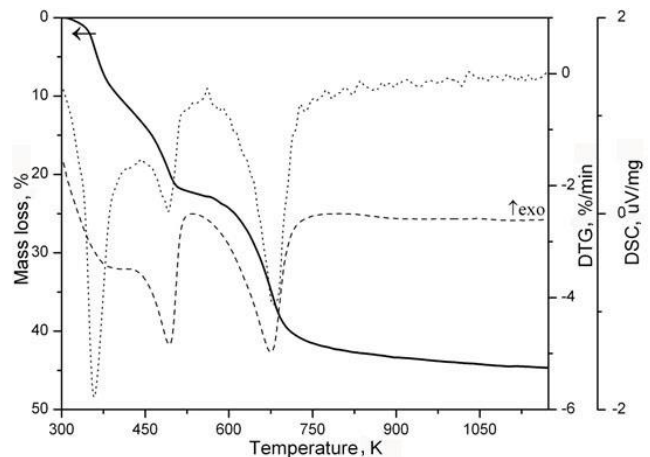


**Fig. 3.** TG (solid line), DTG (dotted line) and DSC (dashed line) curves of as-synthesized Co/Mg/Al LDH

The as-synthesized Co/Mg/Al sample and reconstructed Co/Mg/Al<sub>N293</sub> sample were investigated using the XRF analysis method. The dissolution-crystallization mechanism of mixed oxide regeneration explains the formation of LDHs with new anions and implies a possibility for changing the cation composition of LDHs during the reconstruction process. The proposed formula for the synthesized Co/Mg/Al sample is  $[\text{Mg}_{0.62}\text{Co}_{0.12}\text{Al}_{0.26}(\text{OH})_2](\text{CO}_3)_{0.13} \cdot 0.91\text{H}_2\text{O}$ , where cations and water contents were measured, all other stoichiometric coefficients were calculated. After reconstruction, the results of XRF measurements showed an increase of magnesium concentration in the Co/Mg/Al<sub>N293</sub> specimen. Apparently, the lower amount of cobalt calculated in its formula  $[\text{Mg}_{0.68}\text{Co}_{0.11}\text{Al}_{0.21}(\text{OH})_2](\text{A}^m)_{x/m} \cdot n\text{H}_2\text{O}$  is associated with an increase of Mg content in the material.

A very important characteristic of LDHs is their high specific surface area obtained after thermal treatment. The adsorption of  $\text{N}_2$  gas is often used to evaluate the surface-accessible area and pore size distribution by the Brunauer-

Emmett-Teller (BET) and Barret-Joyner-Halenda (BJH) methods. There is a correlation between the shape of the hysteresis loop and the texture (e.g., pore size distribution, pore geometry, connectivity) of a mesoporous material. An empirical classification of hysteresis loops was given by the IUPAC [28], which is based on an earlier classification by de Boer. The accessible surface is generally that of the internal pores within the crystallites and the external surface between the crystallites. Correspondingly, the measured pores are those inside and between the crystallites. The influence of reconstruction process on the specific surface area and pore size of mixed metal oxides obtained from reconstructed LDHs by heating in air at 923 K were investigated and the results are presented in Table 2 and Table 3.

**Table 2.** Surface area, pore volume and pore diameter of mixed metal oxides obtained from reconstructed LDHs

Surface properties		Samples calcined at 923 K		
		Co/Mg/Al <sub>cal</sub>	Co/Mg/Al <sub>W293</sub>	Co/Mg/Al <sub>W353</sub>
Total surf. calc., m <sup>2</sup> g <sup>-1</sup>	Cylindrical	244.6	128.3	188.4
	Paral. plates	155.2	85.5	125.6
Surface area (BET), m <sup>2</sup> g <sup>-1</sup>		170	94	131
Total pore volume <sup>a</sup> , cm <sup>3</sup> g <sup>-1</sup>		0.365	0.303	0.334
Average pore diam., Å		85.9	128.6	102.3
Max. pore diam. BJH, Å		62.3	100.1	74.1

<sup>a</sup> At p/p<sub>0</sub> = 0.99

**Table 3.** Surface area, pore volume and pore diameter of mixed metal oxides obtained from reconstructed LDHs

Surface properties		Samples calcined at 923 K	
		Co/Mg/Al <sub>N293</sub>	Co/Mg/Al <sub>N353</sub>
Total surf. calc., m <sup>2</sup> g <sup>-1</sup>	Cylindrical	125.9	207.0
	Paral. plates	82.9	129.9
Surface area (BET), m <sup>2</sup> g <sup>-1</sup>		111	145
Total pore volume <sup>a</sup> , cm <sup>3</sup> g <sup>-1</sup>		0.342	0.372
Average pore diam., Å		123.9	102.5
Max. pore diam. BJH, Å		99.4	74.0

<sup>a</sup> At p/p<sub>0</sub> = 0.99

The N<sub>2</sub> adsorption-desorption isotherms of heat-treated cobalt containing LDHs exhibited type IV isotherms with an H1 hysteresis which are characteristic for the mesoporous materials. The t-plot analysis by de Boer method showed the absence of micropores. An increase at high relative pressure indicates interparticle porosity, which seems to show that the formed mixed oxides consist mainly of non-porous nanoparticles within the nanometer range (Fig. 4).

It has been reported that the decomposition of hydroxalclites preserves the overall particle shape and that the surface perpendicular to the basal planes appears cratered [29–32]. Assumption about the shape of the pores can be made on the basis of N<sub>2</sub> adsorption-desorption isotherms (hysteresis), but it also can be determined using different pore models calculations. Thus, experimentally defined specific surface area value should be equal to the value of calculated one when the form of pores is uniform.

The most suitable model of pore shape is the one whose value is the closest to the value of the calculated area. Calculations were made according two models - cylinder pores and pores between parallel plates (Tables 2 and Table 3). The obtained results showed that the parallel plates model suits the description of the pores of reconstructed and calcined LDHs (except the calcined Co/Mg/Al<sub>N293</sub> sample).

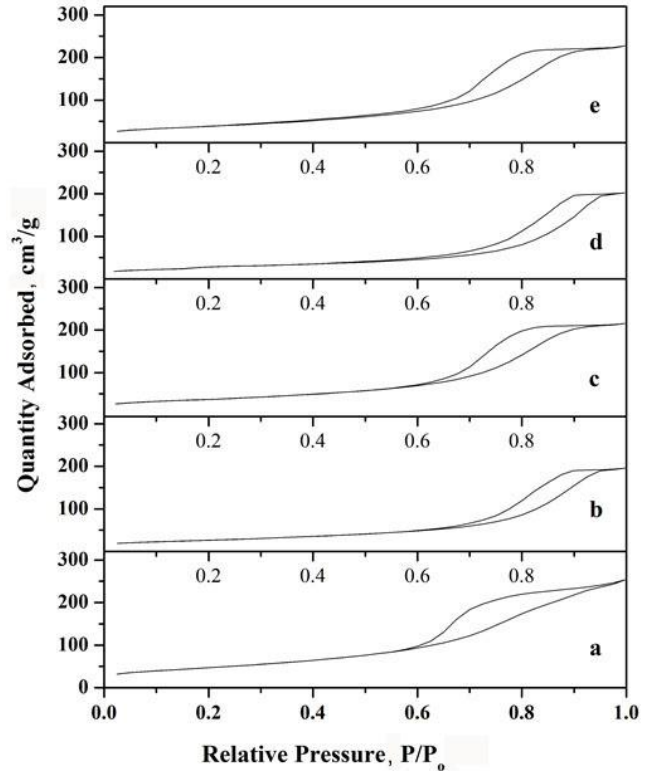


**Fig. 4.** a – adsorption-desorption isotherms for sample Co/Mg/Al<sub>cal</sub>; b – thermally treated at 923 K and reconstructed samples Co/Mg/Al<sub>W293</sub>; c – Co/Mg/Al<sub>W352</sub>; d – Co/Mg/Al<sub>N293</sub>; e – Co/Mg/Al<sub>N353</sub>

The small interparticle porosity occurs due to a “cratering” process. On the other hand, the irregular stacking of plate-like particles creates interparticle pores [33]. The size of these interparticle pores depends mainly on the crystal size; interparticle porosity contributes largely to the total pore volume (Table 2 and Table 3). The pore size distribution for all samples showed one main maximum between 50–130 Å except for Co/Mg/Al<sub>N293</sub> which displayed two maxima at 19 and 100 Å. The mixed oxide samples containing cobalt showed a decrease in total pore volume and an increase of average pore diameter when compared to Co/Mg/Al<sub>cal</sub> material. The chosen process to form mixed oxides (synthesis of LDH – calcination – reconstruction to LDH – second calcination) showed minor effects on pore dimensions. Materials with a high specific surface area were obtained upon decomposition of LDHs irrespective of the starting material [32, 34–36].

The specific surface area of cobalt containing LDHs samples decreased upon reconstruction and calcination from 170 m<sup>2</sup>g<sup>-1</sup> for Co/Mg/Al<sub>cal</sub> to 94 m<sup>2</sup>g<sup>-1</sup> and 131 m<sup>2</sup>g<sup>-1</sup> for Co/Mg/Al<sub>W293</sub> and Co/Mg/Al<sub>W353</sub>, respectively.



Introduction of cobalt into Mg-Al-O mixed oxides lowered the specific surface area [9]. Reformation medium had a considerable influence on the morphology of mixed metal oxides when nitrate solution provided higher specific surface area and higher pore volumes for the same reconstruction temperature. Moreover, a significant increase of specific surface area values were observed for the samples reconstructed in magnesium nitrate solution. Therefore, the better performance of Co/Mg/Al mixed oxides could be achieved [37, 38].

#### 4. CONCLUSIONS

In this study, the influence of the third metal cation on the reconstruction process in layered double hydroxides was investigated. The Co/Mg/Al LDHs were successfully synthesized by the low supersaturation method, thermally decomposed and reconstructed in water or magnesium nitrate media. The XRD measurements provided direct evidence for the phase transformation processes during calcination and reconstruction of layered structures at different temperatures. The partial substitution of the magnesium by cobalt showed changes in the LDHs behaviour during the cycle of synthesis-thermal decomposition-reconstruction. An incomplete regeneration of LDH samples at room temperature in aqueous media has been observed. However, with increasing temperature the reconstruction process of LDHs proceeded to completion. After reconstruction in magnesium nitrate solution the increase of magnesium concentration was observed. It was demonstrated, that the reconstruction medium had a considerable influence on the morphology of mixed metal oxides. The most suitable model of pore shape in reconstructed and calcined cobalt-containing LDH samples was parallel plates model.

#### Acknowledgements

This work was supported by the grant “TUNEABLE Multiferroics based on oxygen Octahedral Structures (TUMOCS)”, from the European Union’s H2020 Marie Skłodowska-Curie Research and Innovation Staff Exchange (MSCA-RISE-2014) programme. Grant Agreement number: 645660. J.P. thanks to the project CEITEC-Central European Institute of Technology CZ.1.05/1.1.00/02.0068 and GACR P207/11/0555 for the financial assistance.

#### REFERENCES

1. **Duan, X., Evans, D.G.** Layered Double Hydroxides. Springer-Verlag Berlin Heidelberg, 2006. <https://doi.org/10.1007/b100426>
2. **Chen, Y.F., Bao, Y., Yang, G.C., Yu, Z.P.** Study on Structure and Photoluminescence of Tb-doped ZnAl-NO<sub>3</sub> Layered Double Hydroxides Prepared by Co-precipitation *Materials Chemistry and Physics* 176 2016: pp. 24–31.
3. **Herrero, M., Benito, P., Labajos, F.M., Rives, V.** Stabilization of Co<sup>2+</sup> in Layered Double Hydroxides (LDHs) by Microwave-Assisted Ageing *Journal of Solid State Chemistry* 180 2007: pp. 873–884. <https://doi.org/10.1016/j.jssc.2006.12.011>
4. **Kannan, S., Swamy, C.S.** Catalytic Decomposition of Nitrous Oxide Over Calcined Cobalt Aluminum Hydrotalcites *Catalysis Today* 53 1999: pp. 725–737.
5. **Klopprogge, J.T., Frost, R.L.** Infrared Emission Spectroscopic Study of the Thermal Transformation of Mg-, Ni- and Co-hydrotalcite Catalysts *Applied Catalysis A-General* 184 1999: pp. 61–71.
6. **Perez-Ramirez, J., Mul, G., Kapteijn, F., Moulijn, J.A.** Investigation of the Thermal Decomposition of Co-Al Hydrotalcite in Different Atmospheres *Journal of Materials Chemistry* 11 2001: pp. 821–830.
7. **Ribet, S., Tichit, D., Coq, B., Ducourant, B., Morato, F.** Synthesis and Activation of Co-Mg-Al Layered Double Hydroxides *Journal of Solid State Chemistry* 142 1999: pp. 382–392. <https://doi.org/10.1006/jssc.1998.8053>
8. **Zhao, M.Q., Zhang, Q., Huang, J.Q., Nie, J.Q., Wei, F.** Layered Double Hydroxides as Catalysts for the Efficient Growth of High Quality Single-Walled Carbon Nanotubes in a Fluidized Bed Reactor *Carbon* 48 2010: pp. 3260–3270.
9. **Mitran, G., Cacciaguerra, T., Loridant, S., Tichit, D., Marcu, I.C.** Oxidative Dehydrogenation of Propane Over Cobalt-Containing Mixed Oxides Obtained from LDH Precursors *Applied Catalysis A-General* 417 2012: pp. 153–162. <https://doi.org/10.1016/j.apcata.2011.12.038>
10. **Cavani, F., Trifiro, F., Vaccari, A.** Hydrotalcite-Type Anionic Clays: Preparation, Properties and Applications *Catalysis Today* 11 1991: pp. 173–301. [https://doi.org/10.1016/0920-5861\(91\)80068-K](https://doi.org/10.1016/0920-5861(91)80068-K)
11. **Liu, X.W., Wu, Y.L., Xu, Y., Ge, F.** Preparation of Mg/Al Bimetallic Oxides as Sorbents: Microwave Calcination, Characterization, and Adsorption of Cr(VI) *Journal of Solid State Chemistry* 79 2016: pp. 122–132. <https://doi.org/10.1007/s10971-016-4018-z>
12. **Vicente, P., Perez-Bernal, M.E., Ruano-Casero, R.J., Ananias, D., Paz, P.A.A., Rocha, J., Rives, V.** Luminescence Properties of Lanthanide-Containing Layered Double Hydroxides *Microporous and Mesoporous Materials* 226 2016: pp. 209–220. <https://doi.org/10.1016/j.micromeso.2015.12.036>
13. **Venugopal, B.R., Shivakumara, C., Rajamathi, M.** A Composite of Layered Double Hydroxides Obtained Through Random Costacking of Layers from Mg-Al and Co-Al LDHs by Delamination-Restacking: Thermal Decomposition and Reconstruction Behavior *Solid State Science* 9 2007: pp. 287–294. <https://doi.org/10.1016/j.solidstatesciences.2007.01.006>
14. **Li, D.L., Ding, Y.Y., Wei, X.F., Xiao, Y.H., Jiang, L.L.** Cobalt-Aluminum Mixed Oxides Prepared from Layered Double Hydroxides for the Total Oxidation of Benzene *Applied Catalysis A-General* 507 2015: pp. 130–138.
15. **Zhou, W.Y., Huang, K., Cao, M.M., Sun, F.A., He, M.Y., Chen, Z.X.** Selective Oxidation of Toluene to Benzaldehyde in Liquid Phase Over CoAl Oxides Prepared from Hydrotalcite-like Precursors *Reaction Kinetics and Mechanisms of Catalysis* 115 2015: pp. 341–353.
16. **Gennequin, C., Cousin, R., Lamonier, J.F., Siffert, S., Aboukais, A.** Toluene Total Oxidation Over Co Supported Catalysts Synthesised Using Memory Effect of Mg-Al Hydrotalcite *Catalysis Communications* 9 2008: pp. 1639–1643. <https://doi.org/10.1016/j.catcom.2008.01.015>

17. **Gennequin, C., Siffert, S., Cousin, R., Aboukais, A.** Co-Mg-Al Hydrotalcite Precursor for Catalytic Total Oxidation of Volatile Organic Compounds *Topics in Catalysis* 52 2009: pp. 482–491.
18. **Gennequin, C., Barakat, T., Tidahy, H.L., Cousin, R., Lamonier, J.F., Aboukais, A., Siffert, S.** Use and Observation of the Hydrotalcite “Memory Effect” for VOC Oxidation *Catalysis Today* 157 2010: pp. 191–197. <https://doi.org/10.1016/j.cattod.2010.03.012>
19. **Bartolo, B.** Advances in Nonradiative Processes in Solids, Plenum Press, New York, 1991. <https://doi.org/10.1007/978-1-4757-4446-0>
20. **Ivanov, M., Klemkaite, K., Khinsky, A., Kareiva, A., Banys, J.** Dielectric and Conductive Properties of Hydrotalcite *Ferroelectrics* 417 2011: pp. 136–142.
21. **Lu, P., Liang, S., Qiu, L., Gao, Y.S., Wang, Q.** Thin Film Nanocomposite Forward Osmosis Membranes Based on Layered Double Hydroxide Nanoparticles Blended Substrates *Journal of Membrane Science* 504 2016: pp. 196–205.
22. **Li, H.J., Su, X.Y., Bai, C.H., Xu, Y.Q., Pei, Z.C., Sun, S.G.** Detection of Carbon Dioxide with a Novel HPTS/NiFe-LDH Nanocomposite *Sensors and Actuators B-Chemical* 225 2016: pp. 109–114. <https://doi.org/10.1016/j.snb.2015.11.007>
23. **Brunauer, S., Emmett, P.H., Teller, E.** Adsorption of Gases in Multimolecular Layers *Journal of American Chemical Society* 60 1938: pp. 309–319.
24. **Cardoso, L.P., Valim, J.B.** Competition Between Three Organic Anions During Regeneration Process of Calcined LDH *Journal of Physics and Chemistry of Solids* 65 2004: pp. 481–485. <https://doi.org/10.1016/j.jpics.2003.08.034>
25. **Baltakys, K., Eisinas, A., Dizhbite, T., Jasina, L., Siauciunas, R., Kitrys, S.** The Influence of Hydrothermal Synthesis Conditions on Gyrolite Texture and Specific Surface Area *Materials Structure* 44 2011: pp. 1687–1701.
26. **Perez-Ramirez, J., Abello, S., Van Der Pers, N.M.** Influence of the Divalent Cation on the Thermal Activation and Reconstruction of Hydrotalcite-like Compounds *Journal of Physical Chemistry C* 111 2007: pp. 3642–3650.
27. **Klemkaite, K., Khinsky, A., Kareiva, A.** Reconstitution Effect of Mg/Ni/Al Layered Double Hydroxide *Materials Letters* 65 2011: pp. 388–391. <https://doi.org/10.1016/j.matlet.2010.10.039>
28. **Lowell, S., Shields, J.E., Thomas, M.A.** Characterization of Porous Solids and Powders: Surface Area, Pore Size and Density, Kluwer Academic Publisher, New York, 2004. <https://doi.org/10.1007/978-1-4020-2303-3>
29. **Reichle, W.T.** Synthesis of Anionic Clay Minerals (Mixed Metal Hydroxides, Hydrotalcite) *Solid State Ionics* 22 1986: pp. 135–141. [https://doi.org/10.1016/0167-2738\(86\)90067-6](https://doi.org/10.1016/0167-2738(86)90067-6)
30. **Reichle, W.T., Kang, S.Y., Everhardt, D.S.** The Nature of the Thermal Decomposition of a Catalytically Active Anionic Clay Mineral *Journal of Catalysis* 101 1986: pp. 352–359.
31. **Jitianu, M., Gunness, D.C., Aboagye, D.E., Zaharescu, M., Jitianu, A.** Nanosized Ni-Al Layered Double Hydroxides-Structural Characterization *Materials Research Bulletin* 48 2013: pp. 1864–1873. <https://doi.org/10.1016/j.materresbull.2013.01.030>
32. **Zhang, Z.Q., Liao, M.C., Zeng, H.Y., Xu, S., Xu, L.H., Liu, X.J., Du, J.Z.** Mg-Al Hydrotalcites as Solid Base Catalysts for Alcoholysis of Propylene Oxide *Fuel Processing and Technology* 128 2014: pp. 519–524.
33. **Valente, J.S., Hernandez-Cortez, J., Cantu, M.S., Ferrat, G., Lopez-Salinas, E.** Calcined Layered Double Hydroxides Mg-Me-Al (Me: Cu, Fe, Ni, Zn) as Bifunctional Catalysts *Catalysis Today* 150 2010: pp. 340–345.
34. **Clause, O., Rebours, B., Merlen, E., Trifiro, F., Vaccari, A.** Preparation and Characterization of Nickel Aluminum Mixed Oxides Obtained by Thermal-Decomposition of Hydrotalcite-type Precursors *Journal of Catalysis* 133 1992: pp. 231–246.
35. **Xia, S.J., Zhang, L.Y., Zhou, X.B., Shao, M.M., Pan, G.X., Ni, Z.M.** Fabrication of Highly Dispersed Ti/ZnO-Cr<sub>2</sub>O<sub>3</sub> Composite as Highly Efficient Photocatalyst for Naphthalene Degradation *Applied Catalysis B-Environmental* 176 2015: pp. 266–277.
36. **Shao, M.M., Jiang, J.H., Xia, S.J., Ni, Z.M., Liu, F.X.** Visible-Light Photocatalytic Degradation Effect of Sn-Contained Layered Double Hydroxides on 4-Chlorophenol *Journal of Inorganic Materials* 31 2016: pp. 27–33.
37. **Zhao, Y., Liang, J., Zhou, X.W.** Synthesis of Carbon Nanotubes by Selective Reduction of Mixed Oxides *Journal of Advanced Materials* 37 2005: pp. 11–15.
38. **Sparks, D.E., Morgan, T., Patterson, P.M., Tackett, S.A., Morris, E., Crocker, M.** New Sulfur Adsorbents Derived from Layered Double Hydroxides I: Synthesis and COS Adsorption *Applied Catalysis B-Environmental* 82 2008: pp. 190–198. <https://doi.org/10.1016/j.apcatb.2008.01.012>